The Mammalian Brain High-Affinity L-Proline Transporter Is Enriched Preferentially in Synaptic Vesicles in a Subpopulation of Excitatory Nerve Terminals in Rat Forebrain

Stephani E. Renick,[1] Dan T. Kleven,[1] June Chan,[3] Katinka Stenius,[4] Teresa A. Milner,[3] Virginia M. Pickel,[3] and Robert T. Fremeau Jr[1,2]

Departments of [1]Pharmacology and Cancer Biology and [2]Neurobiology, Duke University Medical Center, Durham, North Carolina 27710, [3]Department of Neurology and Neuroscience, Cornell University Medical College, New York, New York 10021, and [4]Department of Cell Biology, Yale University School of Medicine, New Haven, Connecticut 06510

The expression of a brain-specific high-affinity Na^+-dependent (and Cl^--dependent) L-proline transporter (PROT) in subpopulations of putative glutamatergic neurons in mammalian brain suggests a physiological role for this carrier in excitatory neurotransmission (Fremeau et al., 1992). To gain insights into potential sites where PROT may function, we used a C-terminal domain antipeptide antibody to determine the regional distribution and subcellular localization of PROT in rat forebrain. PROT immunoreactivity was seen in processes having a regional light microscopic distribution comparable to that of known glutamatergic projections within the cortex, caudate putamen nucleus (CPN), hippocampal formation, and other forebrain regions. In all regions examined by electron microscopy (cortex, CPN, and the stratum oriens of CA1), PROT labeling was observed primarily within subpopulations of axon terminals forming asymmetric excitatory-type synapses. Immunogold labeling for PROT was detected in close contact with membranes of small synaptic vesicles (SSVs) and more rarely with the plasma membrane in these axon terminals. Subcellular fractionation studies confirmed the preferential distribution of PROT to synaptic vesicles. The topology of PROT in synaptic vesicles was found to be inverted with respect to the plasma membrane, suggesting that PROT-containing vesicles are generated by a process involving endocytosis from the plasma membrane. Because PROT lacks any of the known characteristics of other vesicular transporters, these results suggest that certain excitatory terminals have a reserve pool of PROT associated with SSVs. The delivery of PROT to the plasma membrane by exocytosis could play a critical role in the plasticity of certain glutamatergic pathways.

Key words: neurotransmitter transporter; excitatory neurotransmission; L-proline; synapse; electron microscopy; presynaptic nerve terminal; excitatory amino acids

A mammalian brain high-affinity L-proline transporter (PROT) was cloned from a rat forebrain cDNA library, based on amino acid sequence conservation between GABA and norepinephrine transporters (Fremeau et al., 1992). The PROT cDNA encodes a 68 kDa glycosylated protein that exhibits 42–50% amino acid sequence identity with a gene family of Na^+-dependent (and Cl^--dependent) plasma membrane transport proteins that mediate the high-affinity uptake of neurotransmitters (norepinephrine, dopamine, serotonin, GABA, glycine), osmolytes (taurine, betaine), and the metabolite creatine (Shafqat et al., 1993; Miller et al., 1997a). These transporters use transmembrane electrochemical ion gradients to drive active transport of substrates across the plasma membrane and represent critical targets for therapeutic and pathological alterations of synaptic function (for review, see Kanner, 1989; Amara and Kuhar, 1993; Rudnick and Clark, 1993).

The brain-specific expression of PROT in human (Shafqat et al., 1995) and rat (Velaz-Faircloth et al., 1995) tissues is consistent with a unique physiological role for this transporter in the mammalian CNS. The pharmacological specificity, ion dependence, and kinetics of the cloned transporter expressed in nonneural cells (Fremeau et al., 1992, 1996; Shafqat et al., 1995) are similar to the corresponding properties of the high-affinity component of synaptosomal L-proline uptake (Bennett et al., 1972; Peterson and Ragupathy, 1972; Balcar et al., 1976; Nadler, 1987). These properties distinguish PROT from the other widely expressed Na^+-dependent plasma membrane carriers that transport L-proline, including the intestinal brush border "IMINO" carrier (Stevens and Wright, 1985) and the system "A" and system "ASC" neutral amino acid carriers (Christensen, 1990). *In situ* hybridization of rat brain sections and cultured hippocampal neurons revealed that PROT mRNA is expressed by subpopulations of putative glutamatergic neurons in rat brain (Fremeau et al., 1992; Velaz-Faircloth et al., 1995). Subcellular fractionation studies demonstrated that the PROT protein is enriched in synaptosomal membrane fractions, suggesting the targeting of this carrier to presynaptic nerve terminals (Velaz-Faircloth et al., 1995). These findings raise the possibility of a specialized role for PROT and its presumed natural substrate, L-proline, in the modulation of excitatory synaptic transmission in specific excitatory pathways within the CNS. However, there is no direct morphological evidence describing the localization of the PROT protein in mammalian brain.

Received Sept. 11, 1998; accepted Oct. 15, 1998.

This work was supported by National Institutes of Health Grants NS32501 (to R.T.F.), DA04600 and MH40342 (to V.M.P.), and MH42834 and DA08259 (to T.A.M.). We thank Alicia Pohorille for excellent technical assistance and Drs. Reinhard Jahn and Vic Nadler for comments on this project.

Correspondence should be addressed to Dr. Robert T. Fremeau, Jr., Department of Pharmacology and Cancer Biology, Duke University Medical Center, Room C-270 Levine Science Research Center, Medical Center Box 3813, Research Drive, Durham, NC 27710.

To gain insights into potential sites where PROT may function, we examined the regional, cellular, and subcellular localization of PROT in rat forebrain by light and electron microscopic immunocytochemistry and by subcellular fractionation. We show an abundant distribution of PROT in perikarya and processes of the glutamatergic corticostriatal projection system as well as in certain known glutamatergic pathways in the hippocampal formation and other forebrain regions. Furthermore, we provide ultrastructural evidence that the PROT protein is localized to membranes of small synaptic vesicles (SSVs) in a subset of presynaptic axon terminals forming asymmetric "excitatory-type" synapses with dendritic spines in the caudate putamen nucleus (CPN) and the CA1 region of the hippocampus. Subcellular fractionation studies confirmed that the immunoreactive PROT protein is enriched substantially in highly purified synaptic vesicles.

MATERIALS AND METHODS

Antibody production and purification. Polyclonal rabbit antibody A2 was produced and affinity-purified by Research Genetics (Huntsville, AL) against residues 2–18 from the predicted N terminus of rat PROT (KKLQEAHLRKPVTPDLL). A series of immunizations was given, using the peptide synthesized as a multiple antigen peptide (Possnett and Tam, 1989), followed by boosting with a PROT–GST fusion protein. The fusion protein, composed of the N terminus to the beginning of putative transmembrane domain 1 (residues 1–44) of rat PROT, was produced with the pGEX-2T bacterial expression system (Smith and Johnson, 1988). The reactive serum was affinity-purified against the antigenic peptide to yield the final product. The affinity-purified polyclonal antibody directed against the C terminus of rat PROT, antibody C597, has been described previously (Velaz-Faircloth et al., 1995).

Monoclonal antibodies directed against synaptobrevin II [Cl 69.1 (Edelmann et al., 1995)], NMDA receptor R1 subunit [Cl 54.1 (Sucher et al., 1993)], the N-terminal of synaptotagmin [Cl 604.4 (Chapman and Jahn, 1994)], and rabbit polyclonal antiserum against GAT1 [R24 (Pietrini et al., 1994)] were generously provided by Dr. R. Jahn (Max Planck Institute for Biological Chemistry, Department of Neurobiology, AM Fassberg, Goettingen, Germany). A monoclonal antibody recognizing SV2 (Buckley and Kelly, 1985) was donated by Dr. K. Buckley (Department of Neurobiology, Harvard Medical School, Boston, MA). Rat monoclonal antibody against the human dopamine transporter N terminus [Nt.1 (Hersch et al., 1997)] was provided by Dr. A. Levey (Department of Neurology, Emory University School of Medicine, Atlanta, GA). A polyclonal antiserum against EAAC1 (Rothstein et al., 1994) was donated by Dr. J. Rothstein (Department of Neurology, Johns Hopkins University, Baltimore, MD). A monoclonal antibody against synaptophysin (SPV-38) was purchased from Chemicon (Temecula, CA).

Cell culture and transfection. A T_7 vaccinia virus transient expression system (Fuerst et al., 1986) was used to express cDNAs containing the full-length coding sequences of rat PROT (Fremeau et al., 1992), the human dopamine transporter (hDAT) (Giros et al., 1992), the rat GAT1 GABA transporter subtype (Guastella et al., 1990), and the human GlyT1b glycine transporter subtype (Kim et al., 1994) in HeLa cells as described previously (Fremeau et al., 1996). Briefly, HeLa cells ($\sim 5 \times 10^5$ cells/well in six-well plates) were infected with recombinant vaccinia virus strain $VTF_{7\text{-}3}$ (10 pfu/cell) in serum-free Optimem medium (Life Technologies, Gaithersburg, MD), followed 30 min later by liposome-mediated transfection with pBluescript plasmids (Stratagene, La Jolla, CA) containing the indicated transporter cDNA (1 μg/well). At 12 hr after transfection the cells were placed in 1 ml of PBS, pH 7.4, pelleted, and lysed with 0.2 ml PBS/1% SDS.

Tissue preparation. The methods for tissue preparation and immunolabeling were based on those described previously by Leranth and Pickel (1989). For light microscopy, five adult (250–350 gm) male Sprague Dawley rats (Hilltop Lab, Scottsdale, PA) were anesthetized with sodium pentobarbital (150 mg/kg, i.p.) and perfused sequentially through the ascending aorta with 10 ml of heparin solution (1000 U/ml in 0.15 M NaCl), followed by 200 ml of 4% paraformaldehyde in 0.1 M phosphate buffer (PB), pH 7.4. The brains were removed and post-fixed for 30 min in the latter fixative and then incubated overnight in 20% sucrose in PB at 4°C. Sections (40 μm thick) were cut on a freezing sliding microtome and collected in 0.1 M Tris-buffered saline (TBS), pH 7.6, for immunoperoxidase staining.

For electron microscopy, four adult (250–350 gm) male Sprague Dawley rats (Hilltop Lab) were anesthetized with sodium pentobarbital (150 mg/kg, i.p.) and perfused sequentially through the ascending aorta with (1) 10 ml of heparin solution (1000 U/ml in 0.15 M NaCl), (2) 50 ml of 3.75% acrolein (Polysciences, Niles, IL) and 2% paraformaldehyde in PB, and (3) 200 ml of 2% paraformaldehyde in PB. The brains were removed and post-fixed for 30 min in the latter fixative. Sections (40 μm thick) were cut on a vibratome, collected in PB, incubated in a solution of 1% sodium borohydride in PB to remove active aldehydes, and rinsed in PB until bubbles stopped emerging from the tissue (Leranth and Pickel, 1989).

Immunocytochemistry. For immunoperoxidase labeling the anti-PROT antibody was visualized by a modification of the avidin–biotin complex (ABC) method (Hsu et al., 1981). Briefly, free-floating tissue sections were incubated in (1) 1% bovine serum albumin (BSA) in TBS for 30 min, (2) the C597 anti-PROT antibody at a dilution of 1:10,000 for 48 hr at 4°C, (3) a 1:400 dilution of biotinylated goat anti-rabbit IgG (Amersham, Arlington Heights, IL) for 30 min, and (4) a 1:100 dilution of avidin–biotin–peroxidase complex for 30 min. Tissue sections were rinsed between each step with TBS (three times for 10 min each with constant agitation). The peroxidase reaction was developed for 6 min in a solution containing 22 mg of 3,3′-diaminobenzidine (DAB) and 10 μl of 30% H_2O_2 in 100 ml of TBS. For adsorption controls the primary C597 anti-PROT antibody (1:10,000 dilution) was incubated for 16 hr at 4°C with the antigenic peptide (100 nM) (Velaz-Faircloth et al., 1995) before use. Sections prepared for light microscopy were rinsed several times in PB, mounted on glass slides previously coated with gelatin, and dried overnight. They then were dehydrated and mounted under a coverslip with DPX (Aldrich, Milwaukee, WI) for examination, using a Nikon Microphot microscope equipped with bright-field and differential interference contrast optics. Light microscopic identification of brain regions was based on Swanson (1992).

For ultrastructural immunogold silver labeling, the method of Chan et al. (1990) was used to identify the C597 antibody. Briefly, tissue sections were incubated in (1) the C597 anti-PROT antibody at a 1:5000 dilution for 48 hr at 4°C, (2) a 1:50 dilution of colloidal gold-labeled (1 nm) anti-rabbit IgG for 2 hr, and (3) 2% glutaraldehyde in PBS for 10 min. To enhance the size of the gold particles for microscopic detection, we reacted the sections for 4–8 min with a silver solution intense kit (Amersham).

Electron microscopy. Sections prepared for electron microscopy were fixed for 60 min in 2% osmium tetroxide in PB, dehydrated in a series of graded alcohols and propylene oxide, and flat-embedded in Epon 812 between two pieces of Aclar plastic. Ultrathin sections (40–50 nm) were cut through the dorsal CPN, stratum oriens of the CA1 region of the hippocampus, or the deep layers of the somatosensory cortex. These sections were collected from the tissue–Epon interface onto copper mesh grids. The grids were counterstained with lead citrate (Reynolds, 1963) and uranyl acetate for analysis by a Philips 201 electron microscope.

All profiles were categorized (e.g., perikarya, dendrites, axons, and terminals) according to the criteria of Peters et al. (1991). Axon terminals were defined as profiles in which small synaptic vesicles could be seen clearly and that have a cross-sectional diameter of 0.3 μm or greater. Asymmetric synapses were characterized by the greater thickness of the postsynaptic as compared with presynaptic membrane specializations, whereas symmetric synapses had pre- and postsynaptic densities of equal thickness.

Subcellular fractionation. Rat brain synaptic vesicles were purified from isolated nerve terminals essentially as described in Nagy et al. (1976) and Huttner et al. (1983). Briefly, synaptosomes (P2) were purified by differential centrifugation and then lysed by hypotonic shock to release synaptic vesicles and other cytoplasmic organelles. Most large membranes, including synaptic plasma membranes, were removed by centrifugation at 25,000 × *g* for 20 min (LP1). Light membranes, including synaptic vesicles, were collected from the synaptosomal lysate supernatant (LS1) by centrifugation at 165,000 × *g* for 2 hr (LP2). LP2 was purified further by rate-zonal sucrose density gradient centrifugation before a final step of size exclusion chromatography on controlled pore glass (CPG) beads to yield purified synaptic vesicles (Walch-Solimena et al., 1995).

Pronase digestion assay. Digestions were performed essentially as described previously (Johnston et al., 1989). Briefly, 100 μg of rat LP2 membranes was incubated with or without 20 μg of Pronase (Sigma, St. Louis, MO) in 10 mM HEPES/NaOH, pH 7.2, for 20 min at 37°C. Protease inhibitors (final concentrations: 0.5 μg/ml leupeptin, 1 μg/ml aprotinin, 0.7 μg/ml pepstatin, 1 mM EDTA, and 1 mM PMSF) were

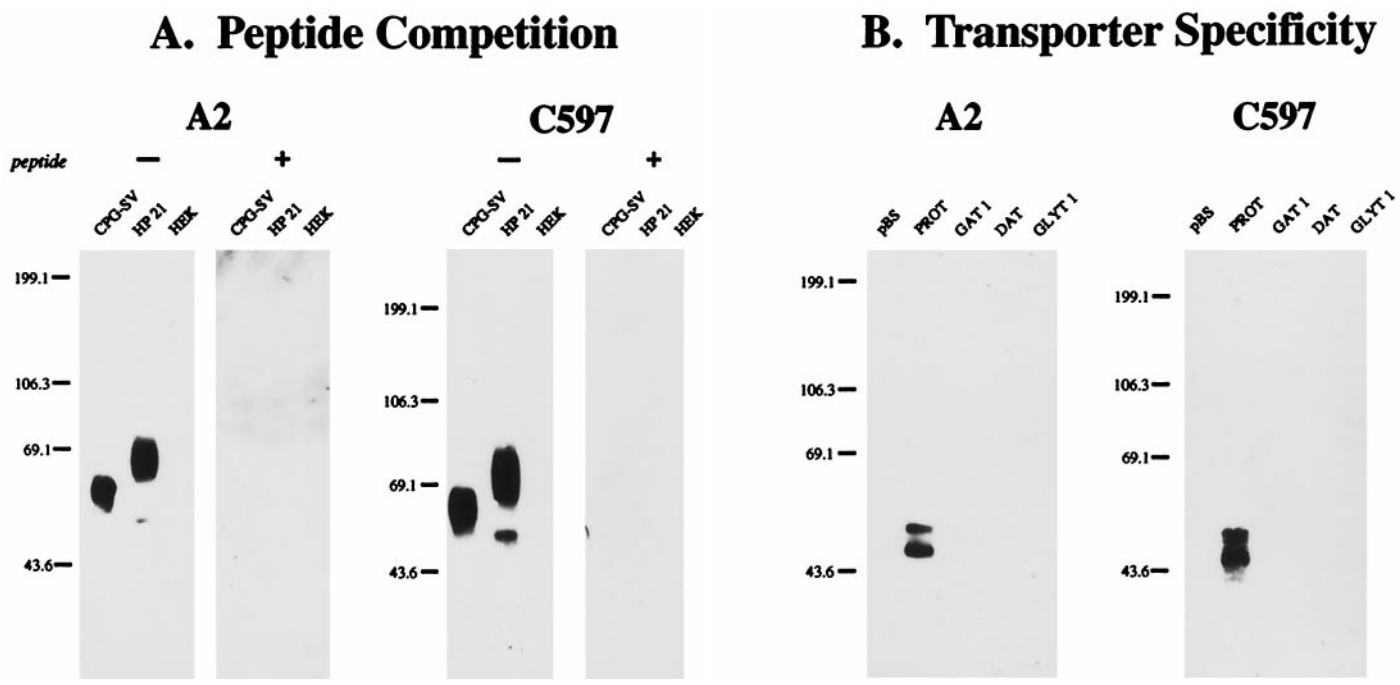

Figure 1. Molecular specificity of the anti-PROT antibodies. *A*, Peptide competition. Membranes from controlled pore glass bead-purified synaptic vesicles (*CPG-SV*), whole-cell detergent lysates of HEK-293 cells stably expressing the rat PROT cDNA (*HP-21*), or untransfected HEK-293 cells (*HEK*) were subjected to SDS-PAGE (8%; 5 μg of protein per lane) and immunoblotted with affinity-purified antibodies directed against the N terminus (*A2*; 1:10,000 dilution) or C terminus (*C597*; 1:40,000 dilution) of rat PROT with (+) or without (−) preabsorption with a 100 nM concentration of the peptide used for its affinity purification. *B*, Transporter specificity. HeLa cells were transfected with the pBluescript II SK$^-$ vector or with the rPROT, rGAT1, hDAT, or hGlyT1b cDNAs. Whole-cell detergent lysates were prepared and subjected to SDS-PAGE (8%; 5 μg of protein per lane) and immunoblotted with the A2 (1:10,000) or C597 (1:40,000) antibodies. The mobilities of prestained protein molecular weight standards are shown on the *left* of each panel in kilodaltons.

added to inactivate the proteases, and the incubation continued for 2 min. A 5× Laemmli SDS-PAGE sample buffer (final concentration: 2% SDS, 1% β-mercaptoethanol, 0.1% bromophenol blue, 10% glycerol, and 50 mM Tris-Cl, pH 6.8) was added, and the samples were incubated for 10 min at 65°C. Ten micrograms of the reaction mixture were loaded per lane for SDS-PAGE and immunoblot analysis.

Deglycosylation assay. Rat LP2 membranes (40 μg) were incubated at 37°C in the presence or absence of detergents (2.5% Nonidet P-40/1% SDS) with 15 U of peptide-*N*-glycosidase F (PNGase F) (Boehringer Mannheim, Indianapolis, IN) in 50 mM $NaPO_4$, pH 7.2, buffer containing 1% β-mercaptoethanol, 10 mM EDTA, and protease inhibitors (2 μg/ml pepstatin, 4 μg/ml leupeptin, and 2.5 mM PMSF). Reactions were terminated at 0, 4, or 16 hr by the addition of 5× SDS-PAGE sample buffer. Samples were heated at 65°C for 10 min before being separated by SDS-PAGE and subjected to immunoblot analysis.

Immunoblot analysis. Membranes were assayed for protein content by the bicinchoninic acid method (Pierce, Rockford, IL) and separated on SDS-polyacrylamide gels, following standard procedures (Laemmli, 1970). Prestained molecular weight standards (Life Technologies, Gaithersburg, MD) were included to provide estimates of protein size. Gels were soaked in transfer buffer (250 mM glycine, 50 mM Tris, and 20% methanol) and electroblotted overnight (50 V, 4°C) to nitrocellulose membranes (Bio-Rad, Hercules, CA). The remaining steps were performed at room temperature. Membranes were incubated for 1 hr in a blocking solution of TBS-T (20 mM Tris-HCl, pH 7.6, 137 mM NaCl, and 0.1% Tween 20) containing 5% nonfat dried milk. Then the blots were rinsed and incubated for 1 hr with the indicated primary antibody diluted in TBS-T. After a washing in TBS-T, horseradish peroxidase-conjugated secondary antibodies against the appropriate species [anti-rabbit Ab, anti-mouse Ab, or anti-rat Ab (Amersham, Buckinhamshire, England)] were diluted 1:5000 in TBS-T and applied for 1 hr. Immunoreactivity was detected by exposure to film (Hyperfilm ECL, Amersham), using enhanced chemiluminescence (ECL; Amersham).

Figure generation. Figures 2–5 were generated from photographic prints captured with an Arcus II desk-top scanner attached to a Power Macintosh 8500/120, using Adobe Photoshop 4.0 and Quark X-Press. Figures 6 and 7 were generated by scanning films with an Apple Color OneScanner (Apple Computers, Cupertino, CA) that used the following software: Ofoto (Light Source Computer Images, Larkspur, CA), Adobe Photoshop (Adobe Systems, Mountainview, CA), and Canvas (Deneba Software, Miami, FL).

RESULTS

Specificity of the anti-PROT antibodies

The specificity of the antibodies used in this study are documented in Figure 1. Affinity-purified antipeptide antibodies directed against the N terminus (A2) or C terminus (C597) of rat PROT recognized a single, broad immunoreactive band centered at ~68 kDa on immunoblots of CPG-purified synaptic vesicles from rat brain (Fig. 1*A*). These antibodies also were immunoreactive against cell lysates prepared from an HEK cell line stably expressing the rat PROT cDNA (HP-21). Two immunoreactive bands were observed on immunoblots of HP-21 lysates probed with the A2 or C597 antibodies: a prominent, broad band centered at ~69 kDa and a minor band at ~53 kDa. Preabsorption of either antibody with the peptide used for its affinity purification abolished all immunolabeling (Fig. 1*A*).

The anti-PROT antibodies also recognized two specific immunoreactive bands on immunoblots of HeLa cells transiently transfected with the rat PROT cDNA: an ~58 kDa band and an ~53 kDa band (Fig. 1*B*). In contrast, no specific immunoreactivity was observed in lysates of HeLa cells transfected with the pBluescript II SK$^-$ vector or with cDNAs encoding several structurally related members of the Na^+-dependent (and Cl^--dependent) transporter family, including the rat GABA transporter subtype, rGAT1 (Guastella et al., 1990), the human dopamine transporter

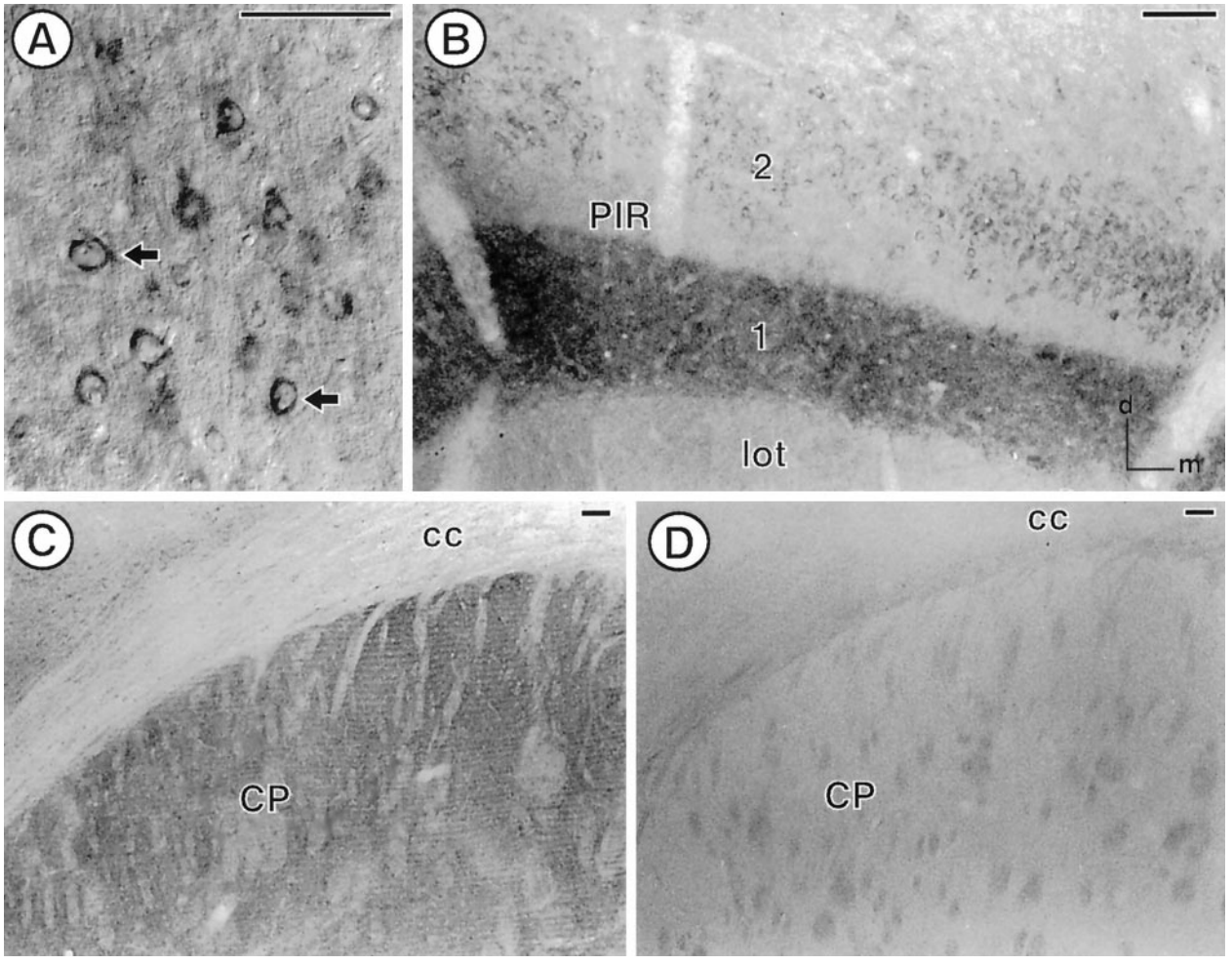

Figure 2. PROT immunoreactivity is found in select regions in the forebrain of the adult rat. *A*, In the somatosensory cortex (corresponding to level 18 in Swanson), PROT immunoreactivity is found in the cytoplasm of perikarya (*arrows*) located in layer 5. *B*, A dense array of PROT-labeled processes is found in layer 1 of the piriform cortex (*PIR*; level 14 in Swanson). Several perikarya with PROT immunoreactivity are found in layer 2, whereas negligible PROT labeling is found in the lateral olfactory tract (*lot*). *C*, In the dorsal quadrant of the caudate putamen nucleus (*CP*), PROT-immunoreactive processes are found in the neuropil surrounding bundles of white matter. *D*, No PROT immunoreactivity is observed in the dorsal caudate putamen nucleus after preadsorption of the antibody with a 100 nM concentration of the cognate peptide. *cc*, Corpus callosum. Scale bar, 100 μm.

(Giros et al., 1992), or the human glycine transporter subtype, hGlyT1b (Kim et al., 1994). These results indicate that the A2 and C597 antibodies react monospecifically with the mammalian brain PROT protein.

The ~53 kDa band observed in both transfected cell lines corresponds to the size of the primary translation product determined by *in vitro*-coupled transcription and translation of the rPROT cDNA in the absence of microsomes (Velaz-Faircloth et al., 1995). The variation in size of the major PROT band observed in native brain tissue versus the cell lines most likely represents differential glycosylation of the primary translation product.

Light microscopic immunocytochemical Localization of PROT

The distribution of PROT in cortical and subcortical structures was similar to that of known glutamatergic pathways (Ottersen and Storm-Mathisen, 1986; Cotman et al., 1987). Immunoperoxidase labeling for PROT was seen prominently in cortical pyramidal neurons (Fig. 2*A*) as well as in punctate, varicose processes in the cortex and throughout the neuropil in the CPN (Fig. 2*C*). No PROT immunoreactivity was detected in adjacent tissue sections that were processed by using the C597 antibody preadsorbed with the 24-amino-acid C-terminal antigenic peptide (Fig. 2*D*). Similarly, there was an absence of labeling in sections that were processed for immunocytochemistry after incubation with preimmune serum (data not shown).

An intense laminar distribution of PROT immunoreactivity was seen in the piriform cortex (Fig. 2*B*) and hippocampal formation (see Fig. 3). Within the cerebral cortex, PROT immunoreactivity was most abundant in the superficial plexiform layer of the piriform cortex, especially layer 1, the outermost portion (Fig. 2*B*). PROT immunoreactivity also was localized to the perikarya of large pyramidal neurons in layer V of the cerebral cortex (Fig. 2*A*). Other neurons that were distributed more widely throughout the cerebral cortex contained comparatively low levels of PROT immunoreactivity. Little or no fiber labeling was observed in myelinated fiber bundles such as the corpus callosum (Fig. 2*C*).

In the hippocampal formation, PROT immunoreactivity showed a distinct, highly laminar labeling pattern that corresponded to a subset of hippocampal glutamate pathways (Bramham et al., 1990). Intense PROT immunolabeling was seen in the

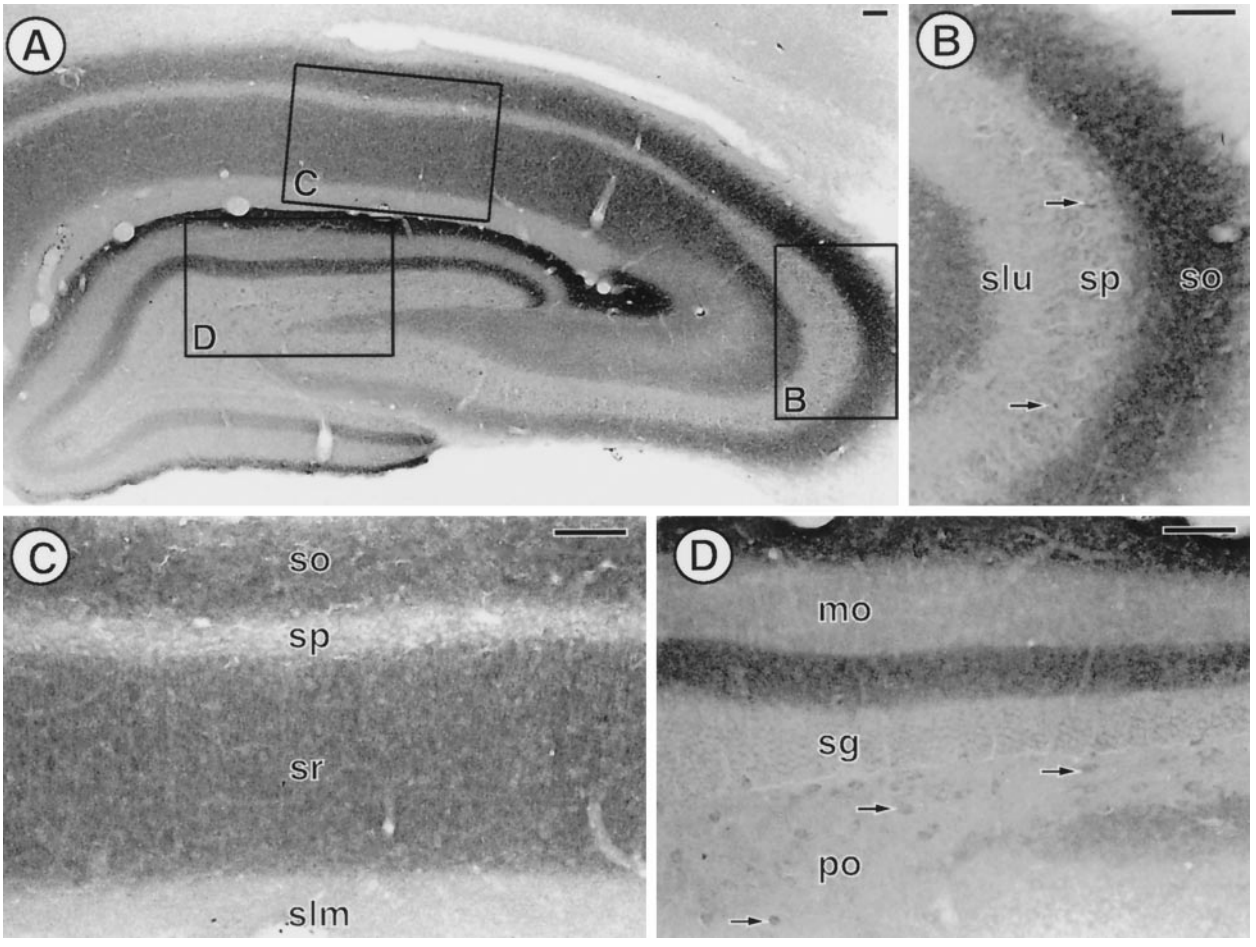

Figure 3. PROT immunoreactivity has a laminar distribution in the adult rat hippocampal formation. *A*, Low-magnification photomicrograph showing the distribution of PROT immunoreactivity in a coronal section of a mid-rostrocaudal level of the hippocampal formation (level 32 in Swanson). *Boxed regions* are enlarged in *B–D*. *B*, In the CA3 region of the hippocampus a dense array of PROT-immunoreactive processes is found in stratum oriens (*so*). A few PROT-labeled perikarya (*arrows*) are observed in stratum pyramidale (*sp*), whereas negligible PROT immunoreactivity is found in stratum lucidum (*slu*). *C*, In the CA1 region of the hippocampus, PROT-immunoreactive processes are densest in strata oriens (*so*) and radiatum (*sr*). *D*, In the dentate gyrus a dense plexus of PROT-immunoreactive processes is found in the inner and outer third of the molecular layer (*mo*). A few PROT-labeled perikarya (*arrows*) are detected in the polymorph layer (*po*). *sg*, Stratum granulosum; *slm*, stratum lacunosum moleculare. Scale bar, 100 μm.

inner and outer thirds of the molecular layer of the dentate gyrus (Fig. 3*A,D*) and in stratum oriens of the CA3 region of the hippocampus (Fig. 3*A,B*). Stratum radiatum of the CA3 subfield and strata oriens and radiatum of the CA1 subfield (Fig. 3*A,C*) were also distinctly, but more modestly, enriched in PROT immunoreactivity. In contrast, stratum lucidum and the middle third of the molecular layer of the dentate gyrus were without detectable immunoreactivity (Fig. 3*A,B,D*). Hippocampal pyramidal and granule cell bodies also were unlabeled (Fig. 3*A–D*). However, modest immunoreactivity was detected in the perikarya of a few interneurons in the hilus of the dentate gyrus (Fig. 3*D*).

PROT localization to membranes of SSVs in specific excitatory-type terminals

The ultrastructural localization of PROT was examined in the deep layers of the somatosensory cortex, CPN, and CA1 region of the hippocampal formation, all of which showed prominent light microscopic labeling. In the somatosensory cortex, peroxidase labeling for PROT was distributed throughout the cytoplasm of neuronal perikarya having the morphological features of pyramidal cells (Peters et al., 1991). In these neurons the reaction product often was localized more intensely to presumed sites of protein synthesis along membranes of the rough endoplasmic reticulum (Fig. 4*A*). The most abundant PROT labeling was seen, however, in unmyelinated axons and axon terminals (Fig. 4*B*). These terminals were 0.2–0.8 μm in diameter and formed one, or sometimes two, asymmetric synapses with small unlabeled dendrites and/or dendritic spines (Fig. 4*B*). The peroxidase labeling within these axon terminals was diffuse but often appeared to rim the membranes of SSVs. Many other axon terminals forming either symmetric or asymmetric synapses and most postsynaptic dendrites were without detectable immunoreactivity (Fig. 4*B*).

Within the CPN and the CA1 region of the hippocampus, PROT was detected primarily in unmyelinated axon and axon terminals. These terminals were 0.2–0.5 μm in diameter and usually formed asymmetric excitatory-type synapses or lacked recognizable membrane specializations within the plane of section (Figs. 5, 6). Terminals with PROT immunoreactivity occasionally contacted more than one postsynaptic target within a single plane of section. As seen in the cortex (see Fig. 4*B*), many other terminals that formed asymmetric axospinous synapses

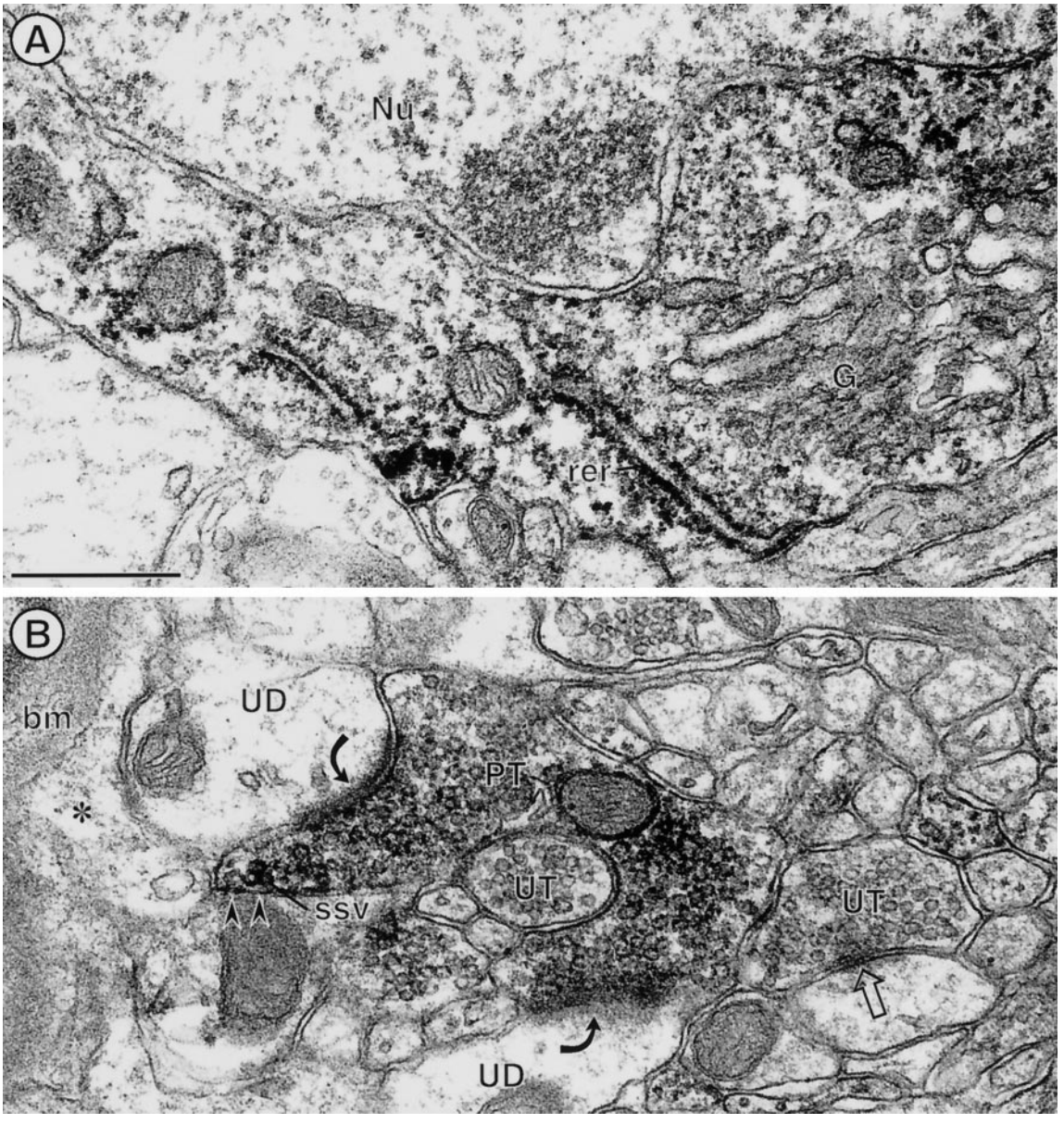

Figure 4. Electron micrographs showing immunoperoxidase labeling for PROT in the cytoplasm of a neuronal perikaryon (*A*) and axon terminal (*B*) within the deep layers of the somatosensory cortex. *A*, The peroxidase labeling is distributed diffusely throughout the cytoplasm surrounding an unlabeled nucleus (*Nu*). The peroxidase product is associated most intensively with saccules of rough endoplasmic reticulum (*rer*). The trans-Golgi lamellae (*G*) show comparatively little immunoreactivity. *B*, PROT immunoperoxidase labeling is seen in a nonuniform distribution throughout an axon terminal (*PT*). Many clusters of small synaptic vesicles (*ssv*) near portions of the plasma membrane (*arrowheads*) that face an astrocytic process (*) also show peroxidase immunoreactivity. This astrocytic process is continuous with the glial profile contacting the basement membrane (*bm*) of a small blood vessel. The labeled terminal forms asymmetric synapses (*curved arrows*) with two separate unlabeled dendrites (*UD*) and also is apposed to another unlabeled axon terminal (*UT*). Scale bar, 0.5 μM.

within the adjacent neuropil were without detectable PROT immunoreactivity in the CPN and CA1 region (Figs. 5*A*, 6*A*). Most postsynaptic dendrites were unlabeled, but as seen in Figure 5*A*, a light diffuse peroxidase reaction product for PROT sometimes was seen within the target dendrites in the CPN.

The vesicular distribution of the peroxidase labeling for PROT in terminals in the CPN and the CA1 region was comparable to that in the somatosensory cortex (Figs. 5*A*, 6*A,B*). In addition, in these latter regions PROT immunogold silver particles were seen frequently in direct contact with the membranes of SSVs (Figs. 5*B*, 6*C*). The labeled vesicles appeared to be equally abundant near the center of the axon terminals and near the plasma membrane. Less frequently, gold labeling for PROT was seen in direct contact with the cytoplasmic surface of the plasma membrane that was apposed by unlabeled neuronal or glial profiles (Fig. 5*B*). PROT labeling rarely was seen near the active zone of the synapse either in vesicles or along portions of the axonal membranes (Fig. 6*C*).

Enrichment of PROT in highly purified synaptic vesicles isolated from rat brain

PROT immunoreactivity was enriched substantially in the highly purified synaptic vesicle fraction (SV) as compared with the synaptic plasma membrane fraction (LP1) (Fig. 7). A similar

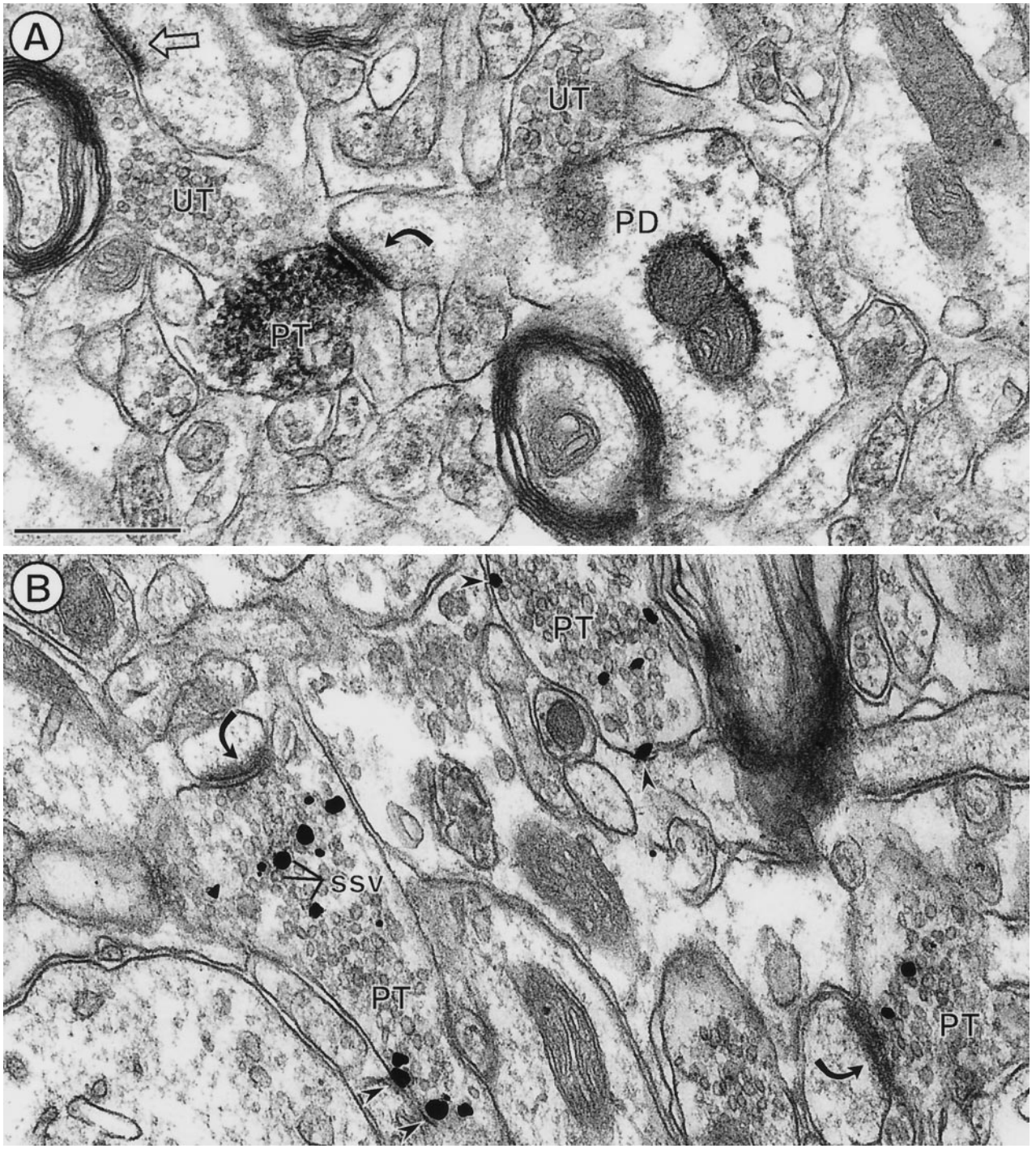

Figure 5. Electron micrographs showing immunoperoxidase (*A*) and immunogold silver (*B*) labeling for PROT in axon terminals (*PT*) in the dorsal striatum. *A*, Immunoperoxidase reaction product (*black precipitate*) is distributed intensely along membranes of small synaptic vesicles (*ssv*) in an axon terminal forming an asymmetric axospinous synapse (*curved arrow*). Sparse labeling also is seen within the dendrite but is absent from other morphologically similar terminals. *B*, Immunogold particles (*straight arrows*) mainly contact membranes of SSVs. Several particles are present along the plasma membrane (*arrowheads*). *UT*, Unlabeled axon terminal. *PD*, Postsynaptic dendrite. Scale bar, 0.5 μM.

distribution pattern was observed for the well characterized synaptic vesicle proteins synaptobrevin II, synaptophysin, and SV2. In contrast, the GAT1 GABA transporter, the dopamine transporter, the EAAC1 glutamate transporter, and the NMDA glutamate receptor proteins were not enriched significantly in the synaptic vesicle fraction. The abundance of PROT in purified synaptic vesicles is consistent with the ultrastructural localization of immunoreactive PROT protein in association with membranes of synaptic vesicles.

Transmembrane topology of PROT in synaptic vesicles

To establish the orientation of the N and C termini of PROT in synaptic vesicles, we determined the susceptibility of the corresponding epitopes to proteolysis. A subcellular fraction enriched

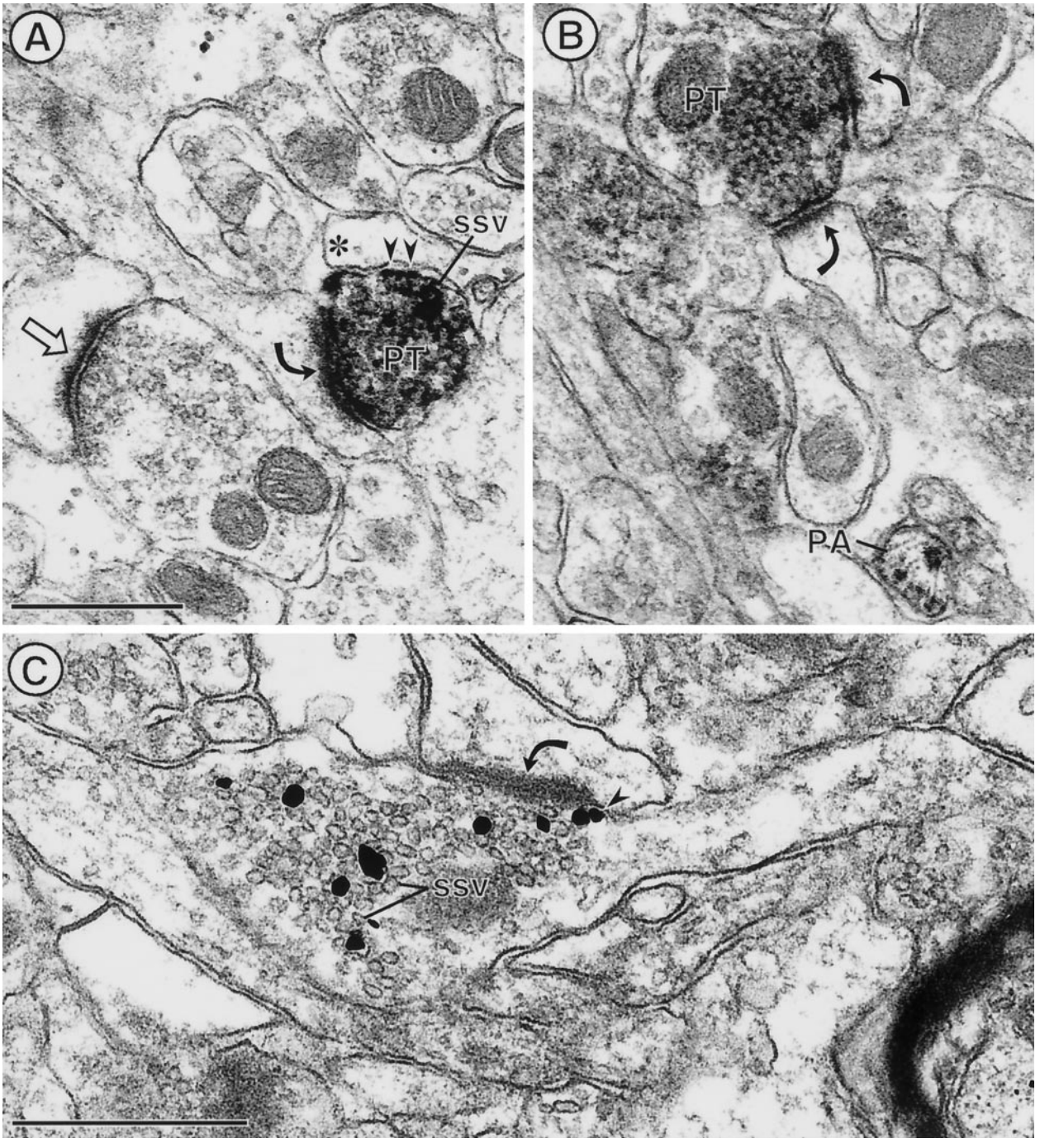

Figure 6. PROT is localized prominently to synaptic vesicles in axon terminals that form asymmetric excitatory-type synapses in the CA1 region of the hippocampal formation (*curved arrows*). In *A* and *B*, peroxidase labeling is distributed intensely throughout the cytoplasm of specific axon terminals (*PT*) that form asymmetric synapses. Certain SSVs, particularly those near the plasma membrane (*small arrows*) apposed to a glial process, appear to be rimmed with peroxidase labeling. *A*, An unlabeled terminal forms a similar asymmetric synapse (*straight arrow*). *B*, A labeled terminal forms dual contacts (*curved arrows*) on two spines. Additionally, a small unmyelinated axon is labeled intensely for PROT (*PA*). Immunogold silver particles in *C* are seen in direct contact with membranes of many SSVs in an axon terminal, forming an asymmetric synapse. One gold particle is also in contact with the plasma membrane (*arrowhead*) adjacent to the synaptic specialization. Scale bar, 0.5 μM.

in synaptic vesicles (LP2) was treated with Pronase, a mixture of endo- and exoproteases, to allow for the digestion of exposed cytoplasmic domains. Then the digests were separated by SDS-PAGE and immunoblotted with the N- or C-terminal anti-PROT antibodies. The epitopes for both the N-terminal (A2) and C-terminal (C597) antibodies were destroyed after proteolysis of synaptic vesicles (Fig. 8*A*). To verify that under these conditions only cytoplasmic domains were digested by Pronase, we used an antibody directed against an intraluminal domain of synaptotagmin, a transmembrane protein of synaptic vesicles with a different topology (Perin et al., 1991). On immunoblots of untreated synaptic vesicles the monoclonal antibody directed against the N terminus of synaptotagmin recognized an ~65 kDa immunoreactive protein. After protease treatment the anti-synaptotagmin

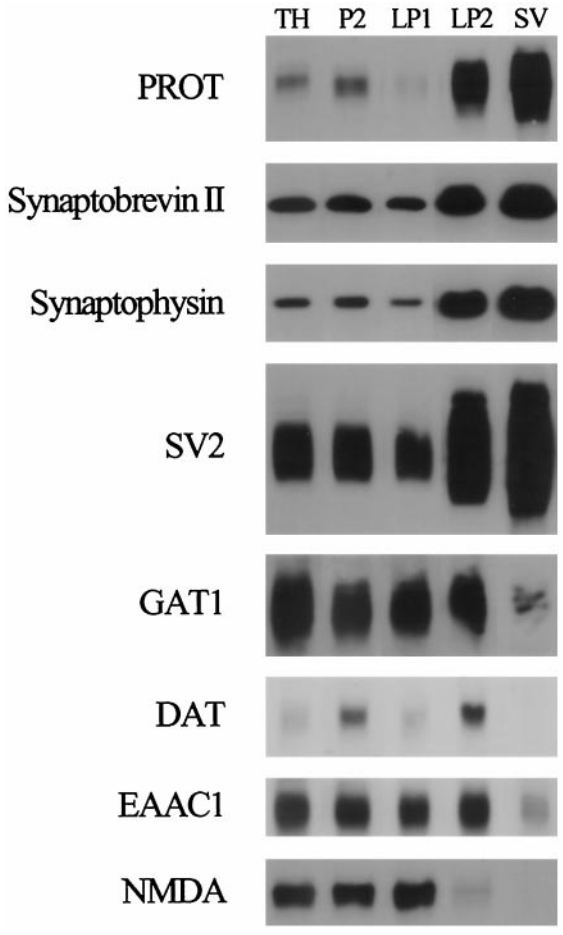

Figure 7. PROT is enriched substantially in highly purified synaptic vesicles. We isolated synaptic vesicles from nerve terminals by subcellular fractionation and monitored the distribution of PROT in the various fractions in comparison to several synaptic vesicle and plasma membrane markers. Briefly, crude synaptosomes (*P2*) were prepared from a rat forebrain homogenate (*TH*) by differential centrifugation and lysed to release synaptic vesicles and other internal membrane compartments. Then most large membranes, including synaptic plasma membranes, were removed by centrifugation at 25,000 × *g* for 20 min (*LP1*). Synaptic vesicles were collected from the synaptosomal lysate supernatant by centrifugation at 165,000 × *g* for 2 hr (*LP2*) and purified further by rate-zonal sucrose density gradient centrifugation and size exclusion chromatography on a controlled pore glass bead column (*SV*). Samples from each subcellular fraction were subjected to SDS-PAGE (5 μg of protein per lane) and immunoblotted with antibodies to the indicated proteins. Note that PROT is enriched substantially in the SV fraction like the synaptic vesicle proteins synaptobrevin II, synaptophysin, and SV2. In contrast, the plasma membrane neurotransmitter transporters and receptors that have been examined are deenriched in the highly purified SV fraction.

antibody recognized an ~23 kDa fragment predicted to contain the transmembrane and luminal domains of the protein (Stenius et al., 1995). These results confirm that the N and C termini of PROT are cytoplasmic in synaptic vesicles.

Next we examined the ability of PNGase F to deglycosylate the putative extracellular/intraluminal loop between transmembrane domains 3 and 4. Previous experiments demonstrated that deglycosylation of rat brain membranes by PNGase F reduced the apparent molecular mass of the mammalian brain PROT protein from ~68 to ~53 kDa, a size that corresponds to the primary translation product (Velaz-Faircloth et al., 1995). Figure 8*B* shows that, in the absence of detergent, little or no deglycosylation of PROT was observed in intact synaptic vesicles over a 16 hr incubation. However, when the synaptic vesicles were solubilized with detergent, significant deglycosylation was observed at 4 hr; by 16 hr the native protein was deglycosylated completely. These results indicate that the glycosylated loop occupies a protected position within the vesicle lumen.

Two lines of evidence confirmed that PNGase F activity does not depend on the presence of detergent. First, the plasma membrane pool of PROT (LP1 fraction), in which glycosylation sites are presumably accessible, could be deglycosylated by PNGase F in the absence of detergent (data not shown). Second, when synaptic vesicles were lysed by repeated freezing–thawing, PNGase F treatment was able to deglycosylate vesicular PROT in the absence of detergent.

DISCUSSION

The present study characterized the distribution of the mammalian brain PROT protein in rat forebrain by preembedding light and electron microscopic immunocytochemistry. In agreement with previous *in situ* hybridization (Fremeau et al., 1992; Velaz-Faircloth et al., 1995) and uptake autoradiography (Nadler et al., 1992) studies, PROT immunoreactivity was localized to specific subpopulations of putative glutamatergic pathways in rat brain, including the corticostriatal, Schaffer collateral commissural, and lateral perforant pathways (Ottersen and Storm-Mathisen, 1986; Cotman et al., 1987). We also obtained the first direct ultrastructural evidence that the PROT protein is localized selectively to a subset of presynaptic axon terminals forming asymmetric excitatory-type synapses typical of glutamatergic terminals in these brain regions (Peters et al., 1991). L-Glutamate is thought to be the principal excitatory transmitter used by the vast majority of excitatory pathways in the mammalian CNS (Fonnum, 1984; Cotman et al., 1987). Our findings support the hypothesis that high-affinity L-proline uptake modulates some aspect of excitatory transmission at specific glutamatergic nerve terminals.

Localization and topography of PROT in membranes of SSVs

The mammalian brain PROT protein was shown by electron microscopy to be localized to SSVs in a selective population of axon terminals forming excitatory-type synapses in several brain regions. Such SSVs are known to participate in fast synaptic transmission at glutamatergic synapses (Südhof and Jahn, 1991; Burns and Augustine, 1995). Furthermore, subcellular fractionation studies confirmed that the immunoreactive PROT protein was enriched substantially in the highly purified synaptic vesicle fraction as compared with the fraction containing synaptic plasma membranes. Thus, on the basis of both morphological and biochemical criteria, the PROT-containing vesicles appear to represent true synaptic vesicles. These results were unexpected, because there is no precedent for the existence of any high-affinity Na^+-dependent uptake process in synaptic vesicles (Maycox et al., 1990).

The topology of PROT in synaptic vesicles was found to be "inverted" with respect to the plasma membrane. The large glycosylated second "extracellular" loop between transmembrane domains 3 and 4 was found to be intraluminal in synaptic vesicles. This orientation is consistent with the hypothesis that the PROT-containing synaptic vesicles are generated by a process involving endocytosis from the plasma membrane. Synaptic vesicles are generated locally in nerve terminals via repeated rounds of exo-

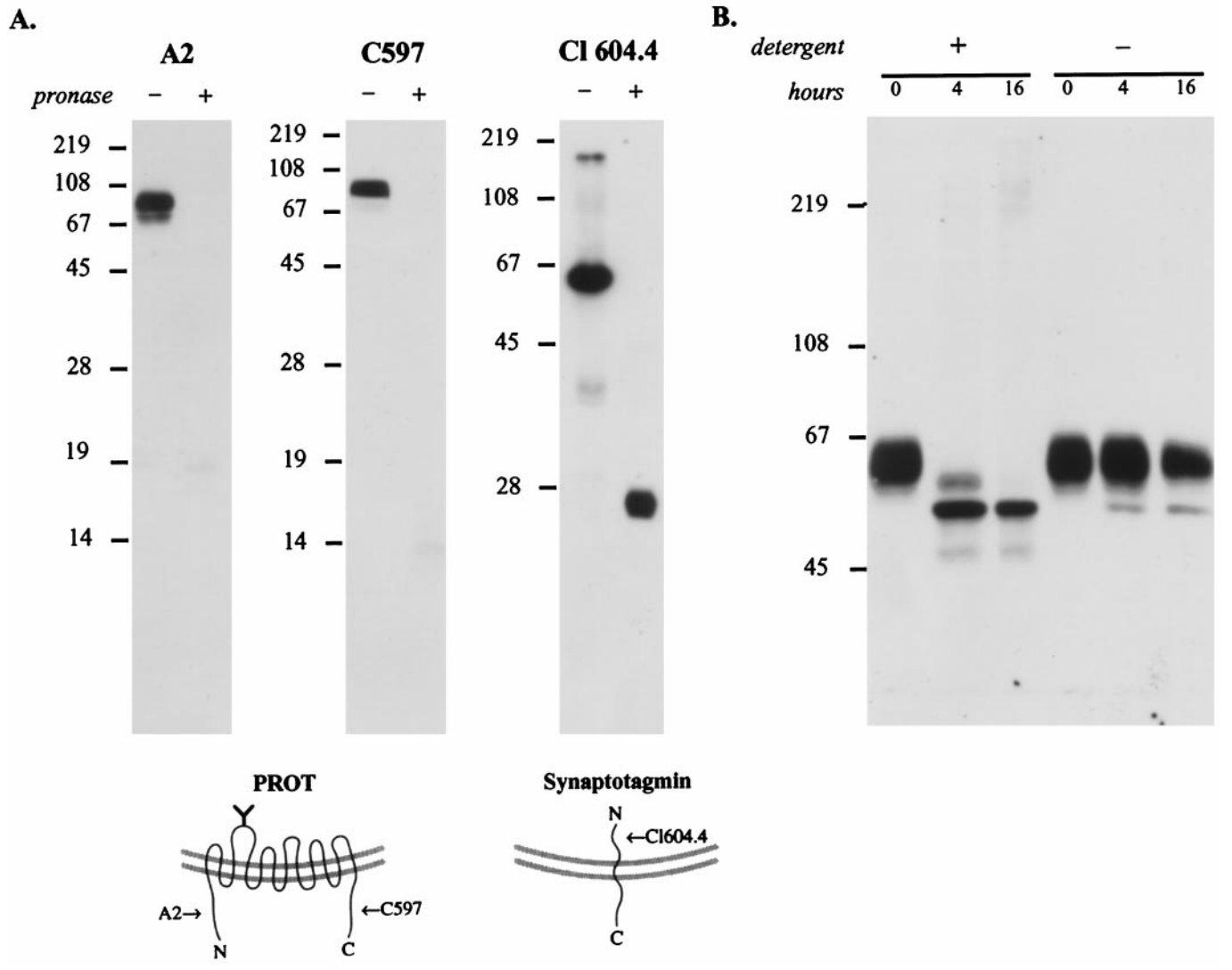

Figure 8. Mapping the topology of PROT in the synaptic vesicle membrane. *A*, PROT N and C termini are oriented cytoplasmically. The location of PROT termini was mapped by subjecting a synaptic vesicle-enriched fraction (LP2) to limited proteolysis. After a 20 min incubation with or without Pronase the samples were separated by SDS-PAGE (15 or 12%) and subjected to immunoblot analysis by using domain-specific antibodies. PROT immunoreactivity is present only in the Pronase-negative reaction when probed with antibodies specific for the N terminus (*A2*; 1:10,000 dilution) or C terminus (*C597*; 1:40,000 dilution), indicating that these structures are present on the external (cytoplasmic) face of the vesicle membrane. In contrast, a monoclonal antibody against the intraluminal N-terminal domain of the integral synaptic vesicle protein synaptotagmin (*Cl 604.4*; 1:1000 dilution) recognized the protected epitope in the partially digested protein. This indicates that during the protease reaction the synaptic vesicles were intact, and loss of PROT immunoreactivity was not attributable to vesicle rupture. The *arrows* in the models indicate the positions of the epitopes of the antibodies used for immunoblotting. *B*, The N-glycosylated loop is intraluminal. A synaptic vesicle-enriched fraction, LP2, was subjected to deglycosylation by PNGase F in the presence or absence of detergents (2.5% NP-40/1% SDS), separated by SDS-PAGE (8%), and immunoblotted with anti-PROT antibody C597 (1:40,000 dilution). In the presence of detergent the native PROT protein is reduced progressively to a single band of ~53 kDa. However, in the absence of detergent a significant loss of glycosylation fails to occur, indicating that the N-linked glycosylation site is located within the vesicle lumen.

and endocytotic recycling between endosomes and the plasma membrane (for review, see Ceccarelli and Hurlbut, 1980; Kelly, 1993; Südhof, 1995). In Figure 9, we model the proposed exo- and endocytotic trafficking of PROT in the nerve terminal on the basis of the classical synaptic vesicle recycling pathway (Heuser and Reese, 1973; Ceccarelli and Hurlbut, 1980). Interestingly, most plasma membrane proteins, including the Na^+/K^+ ATPase and ω-conotoxin-sensitive calcium channels, among others, efficiently are excluded from this compartment during endocytotic recycling (Walch-Solimena, 1995). These results suggest that PROT may contain a synaptic vesicle targeting motif within its primary amino acid sequence. In support of this hypothesis, PROT is targeted to small synaptic-like microvesicles when expressed in PC12 cells (Fremeau et al., 1997).

Several lines of evidence indicate that PROT is not likely to function as a high-affinity Na^+-dependent L-proline transporter in synaptic vesicles. First, there is no significant amino acid sequence identity between PROT and the synaptic vesicle transporters that have been cloned to date, including the vesicular monoamine transporters VMAT1 and VMAT2 (Liu et al., 1992), the vesicular acetylcholine transporter (Alfonso et al., 1993; Erickson et al., 1994; Roghani et al., 1994), and the vesicular GABA transporter (McIntire et al., 1997). Second, the identified synaptic vesicle transporters use a transmembrane electrochemi-

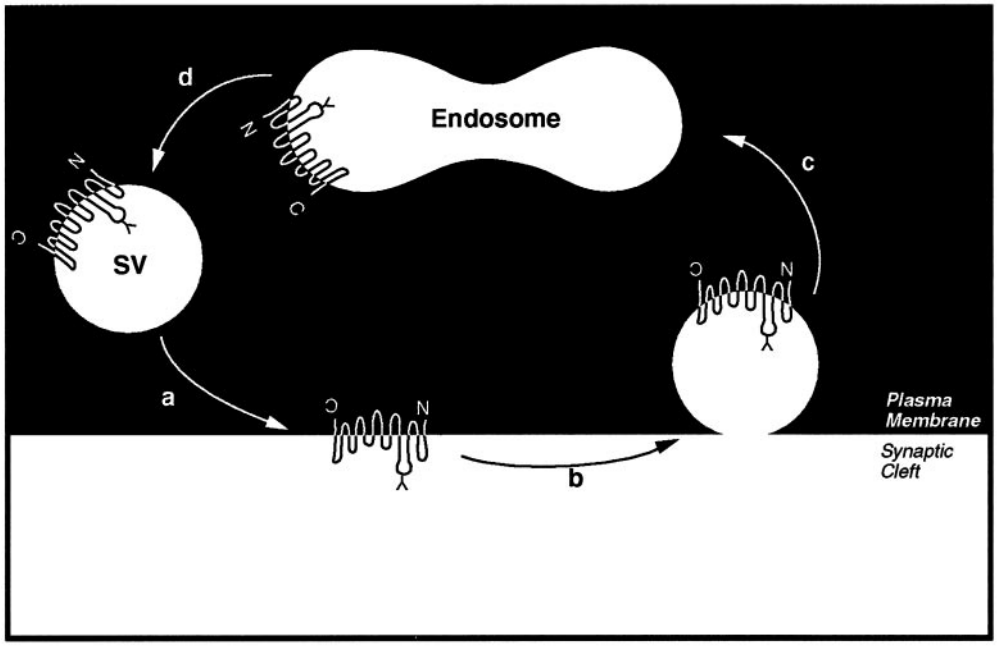

Figure 9. Model depicting the exo-/endocytotic recycling of PROT-containing synaptic vesicles. *a*, According to this model the exocytosis of PROT-containing vesicles in response to a signaling event transiently stimulates high-affinity L-proline uptake into specific excitatory nerve terminals. *b*, Then PROT is retrieved from the nerve terminal membrane by a process that may involve clathrin-dependent endocytosis. *c*, Coated vesicles containing PROT are translocated to early endosomes. *d*, PROT-containing synaptic vesicles are regenerated by budding from endosomes.

cal proton gradient to drive active transport of the transmitter rather than a sodium gradient (for review, see Liu and Edwards, 1997). They also exhibit significantly lower apparent substrate affinities as compared with the cognate plasma membrane transporters. Third, a pH gradient could not drive tritiated L-proline uptake in plasma membrane vesicles prepared from HEK cells stably transfected with rPROT cDNA (Miller et al., 1997b). The possibility cannot be ruled out, however, that PROT may operate as an L-proline transporter with markedly different properties or mediate the uptake and/or exchange of a different substrate in synaptic vesicles.

The PROT-containing vesicles may represent an intracellular reserve pool of high-affinity L-proline transporters that can be recruited to the nerve terminal plasma membrane in response to extracellular signals and/or neuronal activity, thereby increasing high-affinity L-proline uptake into specific excitatory nerve terminals. There are many examples of membrane transport proteins in specialized cell types in the periphery for which the activity is regulated by redistribution from an intracellular endosomal compartment to the cell surface. These include the insulin-regulated GLUT4-facilitated glucose transporter expressed in skeletal muscle and adipocytes (Birnbaum, 1989), the AQP2 water channel of the renal collecting duct (Katsura et al., 1995), and the neutrophil proton pump (Nanda et al., 1996). In each case, specific signaling events induce the dynamic redistribution of intracellular vesicles containing the respective transporter proteins to the cell surface, leading to temporary increases in transport capacity.

Similar mechanisms appear to regulate the high-affinity uptake of neurotransmitters and their precursors into nerve terminals in the mammalian nervous system. For example, potassium depolarization of rat striatal slices stimulates high-affinity Na^+-dependent choline uptake by increasing the number of functional carriers in the nerve terminal plasma membrane (Murrin and Kuhar, 1976; Kuhar and Murrin, 1978; Saltarelli et al., 1987). Similarly, the activation of protein kinase C by phorbol ester treatment in *Xenopus laevis* oocytes expressing GAT1 (Corey et al., 1994; Quick et al., 1997) or HEK cells stably expressing hSERT (Qian et al., 1997) stimulates an increase in the transport capacity for the respective substrates concurrent with an apparent shift in distribution of the transporter protein from intracellular compartments to the plasma membrane. In addition, Davis et al. (1998) observed that multiple signaling pathways regulate the cell surface expression and transport activity of the EAAC1 glutamate transporter subtype in C6 glioma cells. It is unclear which intracellular organelle or organelles participate in the dynamic redistribution of these transporters to the plasma membrane. The present results showing the lack of enrichment of GAT-1 and EAAC1 in the synaptic vesicle fraction indicate that these transporters are not likely to recycle through synaptic vesicles. We did observe, however, abundant immunoreactivity for GAT1, EAAC1, and DAT in the LP2 fraction, which is enriched in intracellular vesicles, including endosomes (see Fig. 7) (Huttner et al., 1983). These results are consistent with the presence of these transporters in specialized populations of recycling endosomes in the nerve terminal that are distinct from synaptic vesicles. The low levels of GAT1 and EAAC1 immunoreactivity observed in the synaptic vesicle fraction may represent a small degree of contamination of this fraction by endosomal fragments and/or by clathrin-coated vesicles that have lost their coat proteins during the subcellular fractionation procedure (see Maycox et al., 1992). Currently, we are attempting to immunoisolate the PROT-containing vesicles to examine the neurotransmitter phenotype and biochemical properties of this unique subpopulation of synaptic vesicles.

Functional implications

Our findings suggest that PROT is one of a small class of proteins that contribute to the molecular heterogeneity of glutamatergic

nerve terminals. These differences in molecular composition presumably reflect differences in the functional regulation of the release and reuptake of transmitters and modulators from specific glutamatergic nerve terminals. High-affinity Na^+-dependent L-proline uptake could modulate excitatory transmission by modifying the extracellular environment and/or by altering the cytoplasmic concentration of its presumed natural substrate, L-proline, at those excitatory synapses that express PROT. On the basis of the flux-coupling stoichiometry of the transporter (Kavanaugh et al., 1992; Miller et al., 1997b), we estimate that the lower limit of extracellular L-proline in the vicinity of the transporter could be <10 nM under standard physiological conditions. Thus, high-affinity uptake may regulate the ability of extracellular L-proline to potentiate excitatory transmission at those synapses that express PROT (Cohen and Nadler, 1997). It also may be important to limit the extracellular L-proline concentration to ensure that it does not reach levels that would activate glutamate and/or strychnine-sensitive glycine receptors inappropriately (Henzi et al., 1992). Alternatively, high-affinity L-proline uptake could serve a novel metabolic role in specific excitatory nerve terminals. It has been suggested that L-proline may serve as a metabolic precursor for glutamate in mouse brain (Johnson and Roberts, 1984), *Drosophila* flight muscles (Hayward et al., 1993), and honeybee retina (Tsacopoulos et al., 1994). Accordingly, high-affinity L-proline uptake could serve to buffer the cytoplasmic glutamate level in specific excitatory nerve terminals. The glutamate produced in this manner could serve as a source of transmitter or enter the Krebs' cycle after conversion to α-ketoglutarate. Future studies are necessary to determine the metabolic fate of the L-proline taken up through mammalian brain PROT.

REFERENCES

Alfonso A, Grundahl K, Duerr JS, Han HP, Rand JB (1993) The *Caenorhabditis elegans unc-17* gene: a putative vesicular acetylcholine transporter. Science 261:617–619.

Amara SG, Kuhar MJ (1993) Neurotransmitter transporters: recent progress. Annu Rev Neurosci 16:73–93.

Balcar VJ, Johnston GAR, Stephenson AL (1976) Transport of L-proline by rat brain slices. Brain Res 102:143–151.

Bennett JP, Logan WJ, Snyder SH (1972) Amino acid neurotransmitter candidates: sodium-dependent high-affinity uptake by unique synaptosomal fractions. Science 178:997–999.

Birnbaum MJ (1989) Identification of a novel gene encoding an insulin-responsive glucose transporter protein. Cell 57:305–315.

Bramham CR, Torp R, Zhang N, Storm-Mathisen J, Ottersen OP (1990) Distribution of glutamate-like immunoreactivity in excitatory hippocampal pathways: a semiquantitative electron microscopic study in rats. Neuroscience 39:405–417.

Buckley K, Kelly RB (1985) Identification of a transmembrane glycoprotein specific for secretory vesicles of neural and endocrine cells. J Cell Biol 100:1284–1294.

Burns ME, Augustine GJ (1995) Synaptic structure and function: dynamic organization yields architectural precision. Cell 83:187–194.

Ceccarelli B, Hurlbut WP (1980) Vesicle hypothesis of the release of quanta of acetylcholine. Physiol Rev 60:396–441.

Chan J, Aoki C, Pickel VM (1990) Optimization of differential immunogold silver and peroxidase labeling with maintenance of ultrastructure in brain sections before plastic embedding. J Neurosci Methods 33:113–127.

Chapman E, Jahn R (1994) Calcium-dependent interaction of the cytoplasmic region of synaptotagmin with membranes. Autonomous function of a single C2-homologous domain. J Biol Chem 269:5735–5741.

Christensen HN (1990) Role of amino acid transport and countertransport in nutrition and metabolism. Physiol Rev 70:43–77.

Cohen SM, Nadler JV (1997) Proline-induced potentiation of glutamate transmission. Brain Res 761:271–282.

Corey JL, Davidson N, Lester HA, Brecha N, Quick MW (1994) Protein kinase C modulates the activity of a cloned γ-aminobutyric acid transporter expressed in *Xenopus* oocytes via regulated subcellular redistribution of the transporter. J Biol Chem 269:14759–14767.

Cotman CW, Monaghan DT, Ottersen OP, Storm-Mathisen J (1987) Anatomical organization of excitatory amino acid receptors and their pathways. Trends Neurosci 10:273–280.

Davis KE, Straff DJ, Weinstein EA, Bannerman PG, Correale DM, Rothstein JD, Robinson MB (1998) Multiple signaling pathways regulate cell surface expression and activity of the excitatory amino acid carrier 1 subtype of Glu transporter in C6 glioma. J Neurosci 18:2475–2485.

Edelmann L, Hanson PI, Chapman ER, Jahn R (1995) Synaptobrevin binding to synaptophysin: a potential mechanism for controlling the exocytotic fusion machine. EMBO J 14:224–231.

Erickson JD, Varoqui H, Schafer MK-H, Modi W, Diebler M-F, Weihe E, Rand J, Eiden LE, Bonner TI, Usdin TB (1994) Functional identification of a vesicular acetylcholine transporter and its expression from a "cholinergic" gene locus. J Biol Chem 269:21929–21932.

Fonnum F (1984) Glutamate: a neurotransmitter in mammalian brain. J Neurochem 42:1–11.

Fremeau Jr RT, Caron MG, Blakely RD (1992) Molecular cloning and expression of a high-affinity L-proline transporter expressed in putative glutamatergic pathways of rat brain. Neuron 8:915–926.

Fremeau Jr RT, Velaz-Faircloth M, Miller JW, Henzi VA, Cohen SM, Nadler JV, Shafqat S, Blakely RD, Domin B (1996) A novel non-opioid action of enkephalins: competitive inhibition of the mammalian brain high-affinity L-proline transporter. Mol Pharmacol 49:1033–1041.

Fremeau Jr RT, Varoqui H, Erickson JD (1997) Mammalian brain PROT is targeted to small synaptic-like microvesicles when expressed in PC12 cells. Soc Neurosci Abstr 23:134.

Fuerst TR, Niles E, Studier FW, Moss B (1986) Eukaryotic transient expression system based on recombinant vaccinia virus that synthesizes bacteriophage T7 RNA polymerase. Proc Natl Acad Sci USA 83:8122–8126.

Giros B, El Mestikawy S, Godinot N, Zheng K, Han H, Yang-Feng T, Caron MG (1992) Cloning, pharmacological characterization, and chromosome assignment of the human dopamine transporter. Mol Pharmacol 42:383–390.

Guastella J, Nelson N, Nelson H, Czyzyk L, Keynan S, Miedel MC, Davidson N, Lester HA, Kanner B (1990) Cloning and expression of a rat brain GABA transporter. Science 249:1303–1306.

Hayward DC, Delaney SJ, Campbell HD, Ghysen A, Benzer S, Kasprzak AB, Costell JN, Young IG, Miklos GL (1993) The *sluggish-A* gene of *Drosophila melanogaster* is expressed in the nervous system and encodes proline oxidase, a mitochondrial enzyme involved in glutamate biosynthesis. Proc Natl Acad Sci USA 90:2979–2983.

Henzi VDB, Reichling SW, Helm SW, MacDermott AB (1992) L-Proline activates glutamate and glycine receptors in cultured rat dorsal horn neurons. Mol Pharmacol 41:793–801.

Hersch SM, Yi H, Heilman CJ, Edwards RH, Levey AI (1997) Subcellular localization and molecular topology of the dopamine transporter in the striatum and substantia nigra. J Comp Neurol 388:211–227.

Heuser JE, Reese TS (1973) Evidence for recycling of synaptic vesicle membrane during transmitter release at the frog neuromuscular junction. J Cell Biol 57:315–344.

Hsu S-M, Raine L, Fanger H (1981) Use of avidin–biotin–peroxidase complex (ABC) in immunoperoxidase techniques: a comparison between ABC and unlabeled antibody (PAP) procedures. J Histochem Cytochem 29:577–580.

Huttner WB, Schiebler W, Greengard P, De Camilli P (1983) Synapsin I (protein I), a nerve terminal-specific phosphoprotein. III. Its association with synaptic vesicles studied in a highly purified synaptic vesicle population. J Cell Biol 96:1374–1388.

Johnson JL, Roberts E (1984) Proline, glutamate, and glutamine metabolism in mouse brain synaptosomes. Brain Res 323:247–256.

Johnston PA, Jahn R, Südhof TC (1989) Transmembrane topography and evolutionary conservation of synaptophysin. J Biol Chem 264:1268–1273.

Kanner BI (1989) Ion-coupled neurotransmitter transport. Curr Opin Cell Biol 1:735–738.

Katsura T, Verbavatz J-M, Farinas J, Ma T, Ausiello DA, Verkman AS, Brown DA (1995) Constitutive and regulated membrane expression of aquaporin 1 and aquaporin 2 water channels in stably transfected LLC–PK1 epithelial cells. Proc Natl Acad Sci USA 92:7212–7216.

Kavanaugh MP, Arriza JL, North RA, Amara SG (1992) Electrogenic

uptake of γ-aminobutyric acid by a cloned transporter expressed in oocytes. J Biol Chem 267:22007–22009.
Kelly RB (1993) Storage and release of neurotransmitters. Cell 72:43–53.
Kim K-M, Kingsmore SF, Han G, Yang-Feng TL, Godinot N, Seldin MF, Caron MG, Giros B (1994) Cloning of the human glycine transporter type 1: molecular and pharmacological characterization of novel isoform variants and chromosomal localization of the gene in the human and mouse genomes. Mol Pharmacol 45:608–617.
Kuhar MJ, Murrin LC (1978) Sodium-dependent, high-affinity choline uptake. J Neurochem 30:15–21.
Laemmli UK (1970) Cleavage of structural proteins during the assembly of the head of bacteriophage T4. Nature 227:680–685.
Leranth C, Pickel VM (1989) Electron microscopic preembedding double immunostaining methods. In: Tract tracing methods 2, recent progress (Heimer L, Zaborsky L, eds), pp 129–172. New York: Plenum.
Liu Y, Edwards RH (1997) The role of vesicular transport proteins in synaptic transmission and neural degeneration. Annu Rev Neurosci 20:125–156.
Liu Y, Peter D, Roghani A, Schuldiner S, Prive GG, Eisenberg D, Brecha N, Edwards RH (1992) A cDNA that suppresses MPP^+ toxicity encodes a vesicular amine transporter. Cell 70:539–551.
Maycox PR, Hell JW, Jahn R (1990) Amino acid neurotransmission: spotlight on synaptic vesicles. Trends Neurosci 13:83–87.
Maycox PR, Link E, Reetz A, Morris SA, Jahn R (1992) Clathrin-coated vesicles in nervous tissue are involved primarily in synaptic vesicle recycling. J Cell Biol 118:1379–1388.
McIntire SL, Reimer RJ, Schuske K, Edwards RH, Jorgensen EM (1997) Identification and characterization of the vesicular GABA transporter. Nature 389:870–876.
Miller JW, Kleven DT, Domin BA, Fremeau Jr RT (1997a) Cloned sodium- (and chloride-) dependent high-affinity transporters for GABA, glycine, proline, betaine, taurine, and creatine. In: Neurotransmitter transporters (Reith MEA, ed), pp 101–150. Totowa, NJ: Humana.
Miller JW, Modjarrad K, Fremeau Jr RT (1997b) Transport properties of the high-affinity L-proline transporter (PROT) determined in membrane vesicles prepared from HEK cells stably transfected with rPROT cDNA. Soc Neurosci Abstr 23:135.
Murrin LC, Kuhar MJ (1976) Activation of high-affinity choline uptake *in vitro* by depolarizing agents. Mol Pharmacol 12:1082–1090.
Nadler JV (1987) Sodium-dependent proline uptake in the rat hippocampal formation: association with ipsilateral commissural projections of CA3 pyramidal cells. J Neurochem 49:1155–1160.
Nadler JV, Bray SD, Evenson DA (1992) Autoradiographic localization of proline uptake in excitatory hippocampal pathways. Hippocampus 2:269–278.
Nagy A, Baker RR, Morris SJ, Whittaker VP (1976) The preparation and characterization of synaptic vesicles of high purity. Brain Res 109:285–309.
Nanda A, Brumell JH, Nordström T, Kjeldsen L, Sengeløv H, Borregaard N, Rothstein OD, Grinstein S (1996) Activation of proton pumping in human neutrophils occurs by exocytosis of vesicles bearing vacuolar-type H^+-ATPases. J Biol Chem 271:15963–15970.
Ottersen OP, Storm-Mathisen J (1986) Excitatory amino acid pathways in the brain. In: Excitatory amino acids and epilepsy (Schwarcz R, Ben-Ari Y, eds), pp 263–284. New York: Plenum.
Perin MS, Johnston PA, Ozcelik T, Jahn R, Francke U, Südhof TC (1991) Structural and functional conservation of synaptotagmin (P65) in *Drosophila* and humans. J Biol Chem 266:615–622.
Peters A, Palay SL, Webster HD (1991) The fine structure of the nervous system. New York: Oxford UP.
Peterson NA, Ragupathy E (1972) Characteristics of amino acid accumulation of synaptosomal particles isolated from rat brain. J Neurochem 19:1423–1438.
Pietrini G, Suh YJ, Edelmann L, Rudnick G, Caplan MJ (1994) The axonal γ-aminobutyric acid transporter GAT-1 is sorted to the apical membranes of polarized epithelial cells. J Biol Chem 269:4668–4674.
Possnett DN, Tam JP (1989) Multiple antigenic peptide method for producing antipeptide site-specific antibodies. Methods Enzymol 178:739–746.
Qian Y, Galli A, Ramamoorthy S, Risso S, DeFelice LJ, Blakely RD (1997) Protein kinase C activation regulates human serotonin transporters in HEK-293 cells via altered cell surface expression. J Neurosci 17:45–57.
Quick MW, Corey JL, Davidson N, Lester HA (1997) Second messengers, trafficking-related proteins, and amino acid residues that contribute to the functional regulation of the rat brain GABA transporter GAT1. J Neurosci 17:2967–2979.
Reynolds ES (1963) The use of lead citrate at high pH as an electron-opaque stain in electron microscopy. J Cell Biol 17:208.
Roghani A, Feldman J, Kohan SA, Shirzadi A, Gundersen CB, Brecha N, Edwards RH (1994) Molecular cloning of a putative vesicular transporter for acetylcholine. Proc Natl Acad Sci USA 91:10620–10624.
Rothstein JD, Martin L, Levey AI, Dykes-Hoberg M, Jin L, Wu D, Nash N, Kuncl RW (1994) Localization of neuronal and glial glutamate transporters. Neuron 13:713–725.
Rudnick G, Clark J (1993) From synapse to vesicle: the reuptake and storage of biogenic amine neurotransmitters. Biochim Biophys Acta 1144:249–263.
Saltarelli MD, Lowenstein PR, Coyle JT (1987) Rapid *in vitro* modulation of [^{3}H]hemicholinium-3 binding sites in rat striatal slices. Eur J Pharmacol 135:35–40.
Shafqat S, Velaz-Faircloth M, Guadano-Ferraz A, Fremeau Jr RT (1993) Molecular characterization of neurotransmitter transporters. Mol Endocrinol 7:1517–1529.
Shafqat S, Velaz-Faircloth M, Henzi VA, Whitney KD, Yang-Feng TL, Seldin MF, Fremeau Jr RT (1995) Human brain-specific L-proline transporter: molecular cloning, functional expression, and chromosomal localization of the gene in human and mouse genomes. Mol Pharmacol 48:219–229.
Smith DB, Johnson KS (1988) Single-step purification of polypeptides expressed in *Escherichia coli* as fusions with glutathione *S*-transferase. Gene 67:31–40.
Stenius K, Janz R, Südhof TC, Jahn R (1995) Structure of synaptogyrin (P29) defines novel synaptic vesicle protein. J Cell Biol 131:1801–1809.
Stevens BR, Wright EM (1985) Substrate specificity of the intestinal brush-border proline/sodium (IMINO) transporter. J Membr Biol 87:27–34.
Sucher NJ, Brose N, Deitcher DL, Awobuluyi M, Gasic GP, Bading H, Cepko CL, Greenberg ME, Jahn R, Heinemann SF, Lipton SA (1993) Expression of endogenous NMDAR1 transcripts without receptor protein suggests post-translational control in PC12 cells. J Biol Chem 268:22299–22304.
Südhof TC (1995) The synaptic vesicle cycle: a cascade of protein–protein interactions. Nature 375:645–653.
Südhof TC, Jahn R (1991) Proteins of synaptic vesicles involved in exocytosis and membrane recycling. Neuron 6:665–667.
Swanson LW (1992) Structure of the rat brain. Amsterdam: Elsevier.
Tsacopoulos M, Veuthey AL, Saravelos SG, Perrottet P, Tsoupras G (1994) Glial cells transform glucose to alanine, which fuels the neurons in the honeybee retina. J Neurosci 14:1339–1351.
Velaz-Faircloth M, Guadano-Ferraz A, Henzi V, Fremeau Jr RT (1995) Mammalian brain-specific L-proline transporter: neuronal localization of mRNA and enrichment of transporter protein in synaptic plasma membranes. J Biol Chem 270:13415–13418.
Walch-Solimena C, Blasi J, Edelmann L, Chapman ER, Fischer von Mollard G, Jahn R (1995) The t-SNAREs syntaxin-1 and SNAP-25 are present on organelles that participate in synaptic vesicle recycling. J Cell Biol 128:637–645.